Open Ceramics 20 (2024) 100666

Contents lists available at ScienceDirect

Open Ceramics

journal homepage: www.sciencedirect.com/journal/open-ceramics

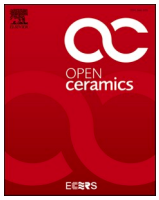

IR-transparent Y_2O_3 ceramics: Effect of zirconia concentration on optical and mechanical properties

Dariia Chernomorets [a,b,*], Pietro Galizia [b], Giacomo Zanetti [c,d], Stefano Varas [c], Alessandro Chiasera [c], Andreana Piancastelli [b], Roman Yavetskiy [a], Jan Hostaša [b]

[a] Institute for Single Crystals of NAS of Ukraine, 60 Nauky Ave., Kharkiv, 61072, Ukraine
[b] CNR-ISSMC, 64 Via Granarolo, 48018, Faenza, RA, Italy
[c] CNR-IFN, CSMFO Lab. and FBK Photonics Unit, Via alla Cascata 56/C, 38123, Povo, TN, Italy
[d] Department of Physics, University of Trento, Via Sommarive 14, 38123, Povo, TN, Italy

ARTICLE INFO

Handling Editor: Jens Guenster

Keywords:
Vacuum sintering
Optical properties
Mechanical properties
Y_2O_3
ZrO_2

ABSTRACT

Y_2O_3 transparent ceramics with different amounts of ZrO_2 were obtained by reactive vacuum sintering at a relatively low temperature of 1735 °C for 22 h. The influence of ZrO_2 concentration within the 0–15 mol.% range on the microstructure, phase composition, microhardness, and optical properties of ceramics in the visible and IR ranges was investigated. SEM and XRD results indicate the absence of secondary phases in the studied concentration range, indicating the formation of single-phase solid solutions. It was shown that doping by ZrO_2 considerably decreases the average grain size of ceramics, while microhardness has the opposite behaviour. 15 mol.% ZrO_2-doped Y_2O_3 ceramics demonstrated the highest transmittance in the visible wavelength range. On the other hand, 5 and 7 mol.% ZrO_2-doped Y_2O_3 could be considered promising materials for the first atmospheric window (3–5 μm).

1. Introduction

Due to transparency in the wide range of wavelengths (0.2–8 μm), good mechanical properties, chemical and thermal stability, and high melting point (2430 °C), yttrium oxide ceramics are widely used in different applications, such as laser-host materials [1–4], IR windows [5,6], nozzles [7], semi-conductor devices [8], etc. One of the most important applications of undoped Y_2O_3 ceramics is IR windows used in the first transparency window (3–5 μm). Compared to other IR-transparent materials, such as spinel, aluminum oxynitride spinel, also known as ALON, or sapphire, Y_2O_3 has the lowest emissivity. The typical requirements for IR windows operating in extreme environments include high transparency, good mechanical properties, and low emissivity [9]. To ensure these properties, ceramics should be fully dense and contain no pores, secondary phases, or impurities, which act as scattering centers due to differences in the refractive index of matrix and defects [10–13]. At the same time, the microstructure of the material should be controlled to obtain ceramics with small grains to improve mechanical properties.

The fabrication process of yttria ceramics is quite challenging due to the high melting point of Y_2O_3, and phase transitions near melting temperature. Utilization of sintering aids allows for a decrease in the sintering temperature and grain size, leading to a fully dense material. Various oxides have been reported as sintering additives for obtaining transparent Y_2O_3, such as Al_2O_3, La_2O_3, ZrO_2, ThO_2, HfO_2, or their combinations [14–22]. Among them, ZrO_2 greatly improves the densification efficiency of yttria ceramics due to the introduction of lattice defects and effective inhibition of grain growth during the sintering process [23].

Nowadays, obtaining Zr-doped Y_2O_3 transparent ceramics by spark plasma sintering (SPS) [24], hot isostatic pressing (HIP) [25,26], vacuum sintering [16,27–30], or their combination [31,32] were reported. Among them, reactive vacuum sintering is a relatively simple approach, offering scalability of production and requiring standard equipment. The typical temperature applied during the vacuum sintering of Y_2O_3 ceramics lies within the 1800–1860 °C range, which is quite high and results in coarse-grained ceramics. A decrease in sintering temperature not only improves processability but also provides much better control of the microstructure and mechanical properties of IR-transparent ceramics. Recently, Z. Yousefian reported transparent Zr-doped Y_2O_3

* Corresponding author. Institute for Single Crystals of NAS of Ukraine, 60 Nauky Ave, Kharkiv, 61072, Ukraine.
E-mail address: chernomorets@isc.kharkov.ua (D. Chernomorets).

https://doi.org/10.1016/j.oceram.2024.100666
Received 30 July 2024; Received in revised form 28 August 2024; Accepted 29 August 2024
Available online 30 August 2024

ceramics obtained by vacuum sintering of commercial nanopowders at a relatively low temperature of 1715 °C [33]. Despite high in-line transmittance at 800 nm, the effect of Zr^{4+} concentration and mechanical properties were not studied by the authors.

Despite the number of papers studying the effect of ZrO_2 on the microstructure and optical properties of yttria ceramics [16,18,28,31,32,34], there is a lack of information on their transmittance in the mid-IR range and mechanical properties in the modern literature. Moreover, different authors provide contradictory information on the optimal concentration of ZrO_2 as a sintering additive in yttria ceramics, probably due to different consolidation approaches used, as well as variation in obtaining temperatures and sources of Zr^{4+} ions. This work aims to study the effect of zirconia concentrations on the optical and mechanical properties of IR-transparent yttria ceramics fabricated by reactive vacuum sintering at low sintering temperature of 1735 °C. A wide range of ZrO_2 concentrations (0–15 mol.%) within the solubility limit equal to 21 mol.% [35], was examined.

2. Materials and methods

2.1. Ceramics fabrication

High-purity commercial powder Y_2O_3 (99.99 %, Nippon Yttrium Co., Ltd., Japan, YT4CP) was used as the starting material and ZrO_2 powder (Tosoh TZ-0Y) was used as a sintering aid (0–15 mol.%). PEG 400 (1 wt. %) was used as a dispersant. The powders were weighed according to the desired stoichiometry (0–15 mol.% of ZrO_2, see Table 1) and ball milled at 300 rpm for 10 h in a zirconia jar with 2 mm zirconia balls in absolute ethanol as solvent. The procedure of powders preparation is described in detail in our previous work [36]. The green bodies with a diameter of d = 20 mm were obtained by uniaxial pressing at 30 MPa and cold isostatic pressing (CIP) at 250 MPa. Calcination in air was performed at 800 °C for 1 h. Afterwards, the ceramics were vacuum sintered at 1735 °C with a soaking time of 22 h. After vacuum sintering, an annealing of the obtained Y_2O_3 ceramics was performed in an air atmosphere at 1100 °C for 1 h. All samples were mirror-polished after sintering and further analyses. The thickness of the samples after polishing ranged from 2.0 to 2.3 mm.

2.2. Characterization of the sintered samples

The microstructure of sintered ceramics was analysed by scanning electron microscopy (SEM, Sigma, Zeiss). The average grain size was calculated using the lineal intercept method by analysing approximately 200 grains for each composition using the following equation: $G = 1.56 \cdot L$, where G is the grain size, and L is the average intercept length. The green density of samples was determined by the geometrical method. The bulk density of vacuum-sintered ceramics was calculated by Archimedes' methods with an accuracy of ±0.5 % according to the C 20–92 ASTM standard [37]. For SEM analysis, polished ceramics samples were thermally etched at 1150 °C for 1 h. The transmittance spectra of the ceramics were obtained with a UV–VIS–NIR spectrometer (Lambda 750, PerkinElmer) and with an FT-IR spectrometer (Nicolet iS5 with the iD1 Transmission accessory, Thermo Scientific) in the 0.25–1.5 μm and 2.5–10 μm wavelengths ranges, respectively.

The phase composition of the bulk sintered samples was analysed with X-ray powder diffractometer Bruker D8 Advance (Theta –Theta vertical goniometer with Bragg Brentano parafocusing geometry) with LINXEYE detector using CuK (alpha) radiation (λ = 1.5418 Å). The analysis was performed in the $10° \leq 2\theta \leq 80°$ range at 2.4°/min scanning rate. The Rietveld refinement method was carried out by using the GSAS-II software [38] in order to refine the lattice constants taking into account microstructural parameters (such as crystallite size and lattice strain). The peak profiles were fitted using the pseudo-Voigt function while a sixth-order polynomial equation was used to fit the background. The Marquardt least-squares procedure was carried out to minimize the difference between the observed and simulated powder diffraction patterns.

Refractive indexes of the samples were measured by m-line spectroscopy at 543.5, 632.8, 1319, and 1542 nm in both transverse electric (TE) and magnetic (TM) polarization using a Metricon mod. 2010 prism coupler instrument (Metriconweb, CarlottoCI). The measurement error is ±0.0005. The Vickers microhardness (H_v) was measured by indentation technique with a Vickers hardness tester (Microdurometer Innovatest Falcon 505, The Netherlands) under an indentation load of 0.2 kg for 10 s at room temperature. Ten measurements were made for every sample and an average value was calculated. To compare the obtained results with literature data presented for the concentration of ZrO_2 in relative at.%, the at.% were recalculated to mol.% based on the $(Y_{1-x}Zr_x)_2O_3$ formula. The at.% notation is generally used to indicate the percentage of Zr^{4+} ions which substitute Y^{3+} and not as the absolute atomic percentage of the compound; as a result, in such case, the ratio between at.% and mol.% is 1:2.

3. Results and discussion

3.1. Microstructure of Y_2O_3 ceramics

Yttrium oxide ceramics doped with ZrO_2 as a sintering aid within the 0–15 mol.% concentration range were obtained by vacuum sintering at 1735 °C for 22 h. The microstructure of mirror-polished samples is shown in Fig. 1. Fig. 1a shows that the Y_2O_3 ceramics with no sintering aids (further marked as Y0Z) were characterized by larger grain size (21.8 ± 2.2 μm) compared to other samples (Fig. 1b). In addition, the Y0Z sample was porous with a pore size in the range of 0.5–3 μm. Pores were present both inside grains and along the grain boundaries of the vacuum-sintered sample, resulting in a relative density of 99.6 %, which is too low to achieve transparency. The theoretical density was calculated from the densities of ZrO_2 and Y_2O_3 as their volume-weighted average.

Since the microstructure of all Zr-doped samples is similar, Fig. 1b shows an SEM micrograph of the Y11Z sample as a representative example. The addition of ZrO_2 as a sintering aid leads to the formation of a more uniform, almost defect-free microstructure. The pore size and concentration decreased significantly compared to the Y0Z sample. This effect is caused by a decrease in grain boundary mobility and more efficient densification during vacuum sintering [23,34,39,40]. According to Yoshida, ZrO_2 suppressed the densification process of Y_2O_3 ceramics [41]. The results obtained in this work indicate the opposite behavior. The relative density of the doped Y_2O_3 ceramics is close to the theoretical values.

Fig. 2 shows the average grain size of the Zr-doped Y_2O_3 ceramics as a function of ZrO_2 concentration. Even 3 mol.% of ZrO_2 is sufficient to considerable inhibit grain growth of yttria ceramics in comparison to the pure Y_2O_3 sample (Fig. 2). This confirms the efficiency of ZrO_2 as a sintering aid. The average grain size of the doped ceramics (Y3Z-Y15Z) was in the range of 6.0–7.8 μm, which is much lower compared to that reported in Ref. [34]. This difference can be attributed to the lower sintering temperature of yttria ceramics obtained in our work. No secondary phases at the grain boundaries are observed by SEM within the whole concentration range studied (up to 15 mol.% of ZrO_2), indicating that the solubility limit was not reached.

Table 1
Compositions of ZrO_2-doped Y_2O_3 samples.

Sample	Y0Z	Y3Z	Y5Z	Y7Z	Y9Z	Y11Z	Y13Z	Y15Z
c(ZrO_2), mol.%	0	3	5	7	9	11	13	15

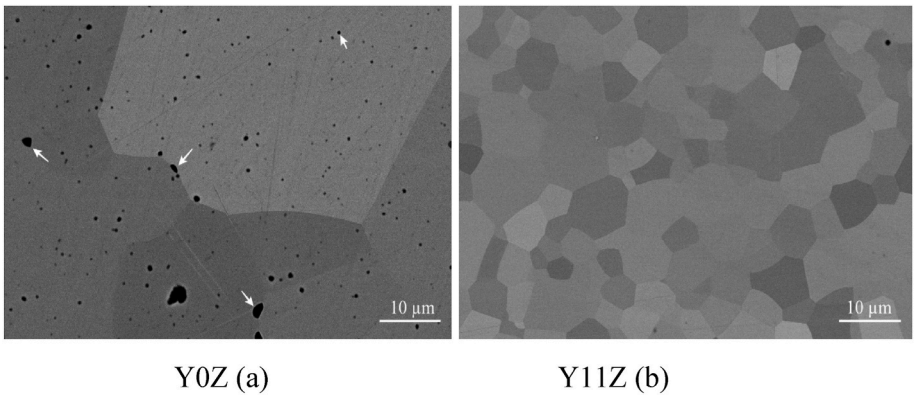

Fig. 1. SEM pictures (micrographs) of Y0Z (a) and Y11Z (b) ceramics obtained by vacuum sintering at 1735 °C for 22 h; arrows indicate pores.

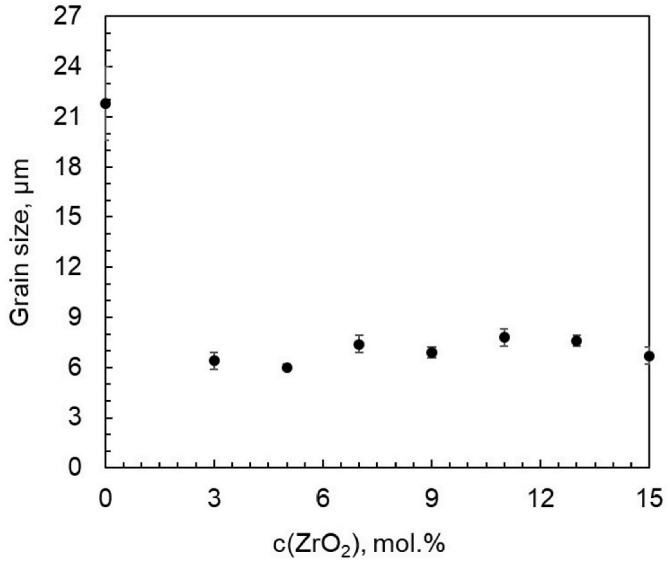

Fig. 2. Average grain size of ZrO_2-doped Y_2O_3 ceramics vs. ZrO_2 doping concentration.

3.2. XRD: phase composition and lattice parameters of ZrO_2-doped Y_2O_3 ceramics

XRD analysis of bulk samples of Y_2O_3 ceramics doped with a different content of ZrO_2 is presented in Fig. 3. Regardless of the ZrO_2 concentration, all the samples crystallize in a cubic structure with Ia-3 space group corresponding to JCPDS card No. 41–1105. There are no extra peaks from secondary phases even at the highest ZrO_2 concentration of 15 mol.%. X. Hou reported precipitation of secondary phases on the grain boundaries in 4 at.% ZrO_2-doped Y_2O_3 ceramics [18]. In our case, no secondary phases were detected by XRD and SEM in 15 mol.% (7.5 at. %) of ZrO_2-doped yttria, in good agreement with the ZrO_2–Y_2O_3 phase diagram [35]. Variations in the solubility range can be caused by differences in the cooling rate during sintering of ceramics. The slight shift of the peaks observed in Fig. 3 is caused by a change in the lattice parameters with different sintering aid concentrations. Since Zr^{4+} ions substitute Y^{3+} ions in the Y_2O_3 crystal lattice, doping with ZrO_2 caused the formation of point defects in ceramics. They improve densification and diffusion during vacuum sintering, as well as the final properties of the obtained material [39].

Lattice parameters of bulk Y_2O_3 samples were calculated using the Rietveld method and are presented in Table 2 along with the available literature data for the same compositions. Since the ionic radius of Zr^{4+} (0.72 Å) is smaller in comparison with Y^{3+} (0.90 Å), the doping leads to a decrease of the yttria lattice constant with an increase in ZrO_2 concentration. There are non-linear changes in the lattice parameters of Y_2O_3 ceramics. A non-linear trend has already been observed in the Tb_2O_3-ZrO_2 and Y_2O_3-ZrO_2 systems [34,42]. First of all, it can be explained by the morphology of the initial materials, in particular, ZrO_2 powders. Since the starting powders were agglomerated it is possible that in some samples, such as Y7Z, ZrO_2 did not fully take part in the formation of a solid solution and incomplete replacement of Y^{3+} by Zr^{4+} ions occurred. Thus, the formation of the secondary Zr-containing phase, such as $Zr_3Y_4O_{12}$, is possible during the cooling down of the ceramics after vacuum sintering [35,43,44]. The quantities of secondary phases can be quite small, within the XRD method measurement error.

Another explanation of non-linear changes of yttria lattice parameters comes from different charge compensation mechanisms during solid-solution formation, accompanied by different changes in specific volume of defects [39]:

$$2ZrO_2 + 2Y_Y^X \Leftrightarrow 2Zr_Y^{\bullet} + O_i'' + Y_2O_3, 1.3\ \text{eV}\ \left(+0.04\ \text{Å}^3\right) \quad (1)$$

$$3ZrO_2 + 4Y_Y^X \Leftrightarrow 3Zr_Y^{\bullet} + \dddot{V}_Y + 2Y_2O_3, 2.0\ \text{eV}\ \left(-0.05\ \text{Å}^3\right) \quad (2)$$

In equations (1) and (2), according to the Kröger-Vink notation [45], Y_Y^X means Y ions occupying Y site with a zero effective charge; $Zr_Y^{\bullet}$ denotes positive charged Zr occupying the Y site; O_i'' is negatively charged O in interstitial position; $\dddot{V}_Y$ denotes triple negative charged yttrium vacancy.

Taking into account the wide range of the ZrO_2 concentrations studied, it could be assumed that some deviations from the predicted solubility mechanism occur. As a result, the formation of different charge-compensating defects for Y_2O_3 doped with Zr^{4+} may cause a non-linear change in the lattice parameter of ceramics, especially for high doping levels (see Refs. [34,42]). Moreover, the formation of more complex defects involving several Zr^{4+} ions cannot be excluded, which was not considered in the calculations. Nevertheless, the measured values are generally in line with the data presented in the literature.

3.3. Mechanical properties

Excellent mechanical properties are important for a wide range of applications of transparent ceramic materials [1,48,49]. The Vickers microhardness of the Y_2O_3 ceramics doped with various concentrations of ZrO_2 was tested under an indentation load of 0.2 kg. Fig. 4 presents the influence of the ZrO_2 amount on the Vickers microhardness H_v of the analysed samples. The increase in ZrO_2 concentration leads to a steady increase of microhardness from 7.1 GPa for pure Y_2O_3 to 10.3 GPa for the Y15Z sample. Obtained values are higher than those reported by X. Li (7.57–8.95 GPa) in the 0–10 at.% range of ZrO_2 concentration [32].

The increase of Vickers microhardness of yttria ceramics may be

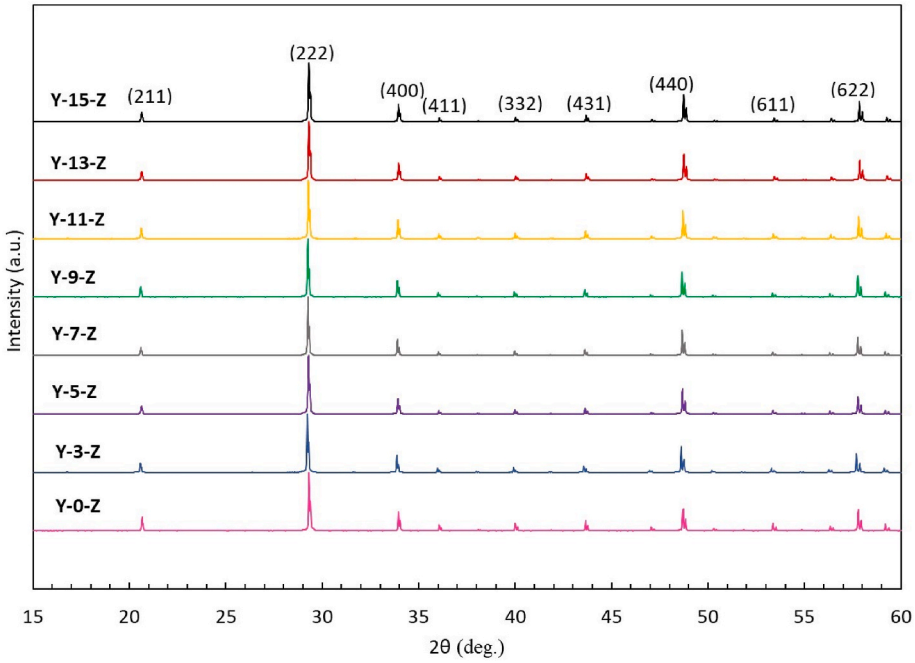

Fig. 3. X-ray diffraction patterns of Y_2O_3 ceramics doped with different ZrO_2 concentrations.

Table 2
Lattice parameters of ZrO_2-doped Y_2O_3 ceramics as a function of ZrO_2 concentration.

Sample	a, Å	a, Å (Literature data)
Y0Z	10.5927	10.6039–10.6118 [31,46,47]
Y3Z	10.5865	
Y5Z	10.5892	10.5948–10.5973 [16,31]
Y7Z	10.5908	
Y9Z	10.5765	10.5841 [16]
Y11Z	10.5832	
Y13Z	10.5733	
Y15Z	10.5702	

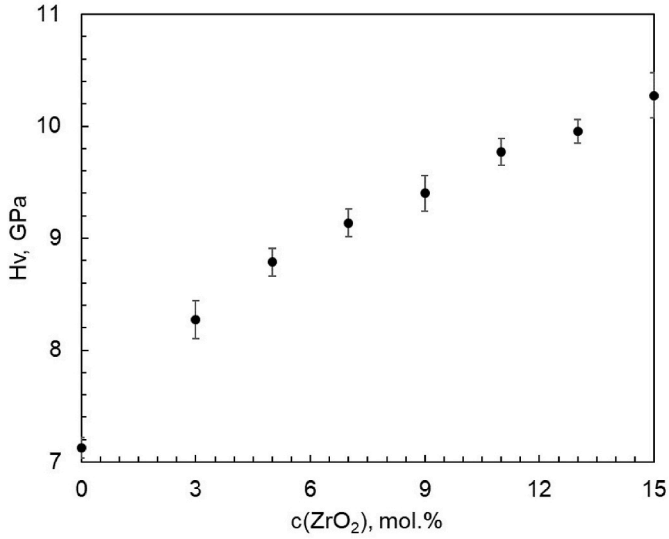

Fig. 4. Vickers microhardness of Y_2O_3 ceramics doped with different ZrO_2 concentrations.

connected with a decrease in the lattice parameters due to the substitution of Y^{3+} ions with Zr^{4+} ions in the crystal structure during the vacuum sintering. On the other hand, the grain size did not change significantly with different concentrations of the sintering aid within the 3–15 mol.% ZrO_2 concentration, indicating that the Hall-Petch effect was not observed. Hence, only the composition of the samples influenced their mechanical properties. The presence of ZrO_2 additives in yttria ceramics introduces minor distortions of its crystal lattice. These distortions prevent plastic flow within the grain, contributing to an increase in the hardness values of ceramics. The increase in the hardness values of yttria ceramics is actually proportional to the change in the crystal lattice parameters caused by the presence of ZrO_2 additives [50]. Thus, yttrium oxide ceramics with high concentrations of ZrO_2 can be useful for applications where both high transparency and high microhardness are required simultaneously.

3.4. Optical properties

The refractive index dependence of analysed samples on wavelength is presented in Fig. 5. Refractive index measurements were done at 543.5, 632.8, 1319, and 1542 nm for all the prepared compositions. The results obtained for TE and TM measurements were very close, and thus average values are presented. An expected decrease in the refractive index values with increasing wavelengths was observed for all the studied samples. The value of the refractive index has an additive character as long as a single-phase solid solution of ZrO_2 in Y_2O_3 is formed.

Fig. 6a shows changes in the refractive index of analysed Y_2O_3 ceramics with different concentrations of ZrO_2. An increase in the amount of sintering aid leads to a linear increase of refractive index values at 1319 nm from 1.8838 to 1.9048 for Y0Z and Y15Z, respectively. This effect occurs because of higher values of the refractive index of pure ZrO_2 compared to pure Y_2O_3 [51,52]. Changing the material's refractive index leads to a change in the theoretical in-line optical transmittance. Using the formula $T_{max} = 2n/(1+n^2)$, the values of the maximal in-line transmittance at 632.8 and 1319 nm were calculated based on the measured refractive index data. Fig. 6b shows the dependence of the T_{max} at 632.8 and 1319 nm on ZrO_2 concentration in Y_2O_3 ceramics. Since transmittance depends on the refractive index of the material, an

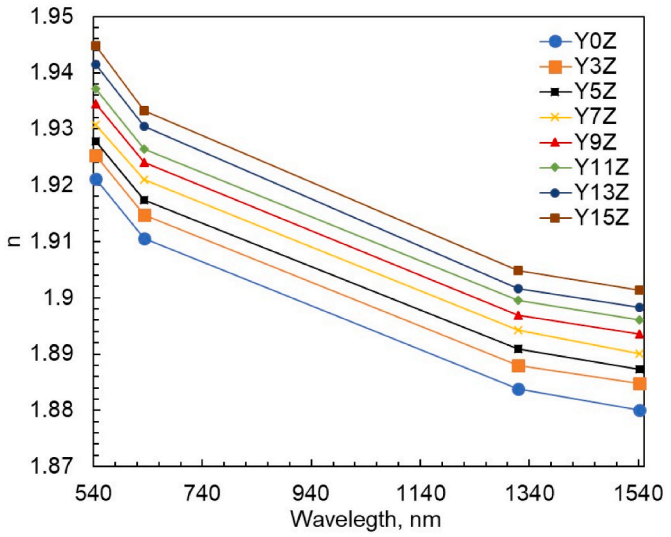

Fig. 5. Dependence of refractive index of ZrO_2-doped Y_2O_3 ceramics on wavelength; the presented data are average values calculated from the TE and TM measurements; the lines are shown just to guide the eye.

increase in ZrO_2 amount leads to a decrease in T_{max} values.

Fig. 7 shows the appearance of vacuum-sintered and polished Y_2O_3 ceramics doped with different concentrations of ZrO_2. It can be seen that the Y0Z sample is translucent, while doping by ZrO_2 has a drastic effect on the transparency of ceramics, in good agreement with their microstructure revealed by SEM (Fig. 1). Y3Z-Y15Z samples demonstrate good optical quality, while Y13Z and Y15Z seem to be the most transparent.

The in-line transmittance of the vacuum-sintered Y_2O_3 samples measured at room temperature is shown in Fig. 8. Y7Z, Y13Z, and Y15Z samples demonstrate high in-line transmittance in the visible wavelength range, close to the theoretical values. The optical properties of these ceramics are comparable, but Y15Z exhibited the highest transmittance, which is 77 % at 633 nm, 80.4 % at 1319 nm, and 83.5 % at 5 μm (94.3 %, 97.7 %, and 99.5 % of the theoretical values, respectively). The optimal ZrO_2-doping concentration of 15 mol.%, obtained in this work, is much higher than 3–5 mol.% typically reported in the literature [16,27,34]. Moreover, the sintering temperature for highly transparent Y_2O_3 ceramics is typically 1800–1860 °C, which is higher than the 1735 °C used in this work. It seems that a higher sintering temperature leads to the formation of a higher equilibrium concentration of defects in the material, thus a lower amount of sintering aid is required to obtain fully-dense ceramics. In our case, a larger doping level should be used to achieve the same sinterability at a much lower temperature. Further increase in zirconia amount probably would lead to the deterioration of the optical properties of Y_2O_3 ceramics due to the proximity to the solubility limit. It should be noted that Y15Z ceramics demonstrate both excellent transparency and Vickers microhardness.

Fig. 8b shows the in-line transmittance of yttrium oxide ceramics in the IR wavelength range. Transmittance of the samples increased since the effect of small-sized defects on the optical properties is lower at longer wavelengths [12]. In the first atmospheric window (3–5 μm) Y5Z and Y7Z ceramics may be of great interest, also considering their higher thermal conductivity [32].

4. Conclusions

The effect of ZrO_2 concentration on the microstructure, phase composition, and optical and mechanical properties of Y_2O_3 transparent ceramics obtained by vacuum sintering at 1735 °C for 22 h was studied. An increase in the ZrO_2 concentration results in a decrease in the lattice parameters due to different ionic radii of Y^{3+} and Zr^{4+}. Non-linear changes in the lattice constant can be caused by the formation of different charge-compensating defects or defect complexes in the yttria ceramics. No secondary phases were observed by SEM and XRD methods in any of the vacuum-sintered ZrO_2-doped Y_2O_3 ceramics, indicating that the solubility limit was not reached. The formation of a single-phase solid solution within the whole composition range studied is also supported by the linear increase of the refractive index of ceramics.

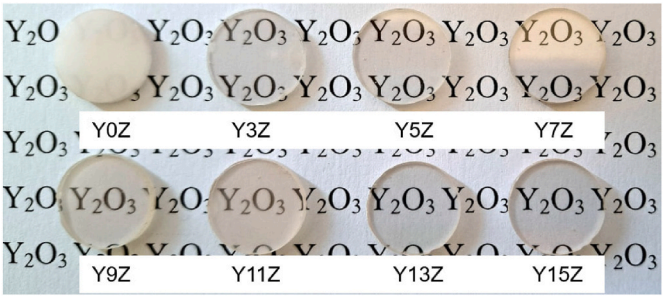

Fig. 7. Appearance of annealed and polished ZrO_2-doped Y_2O_3 ceramics doped with different concentrations of ZrO_2 obtained by vacuum sintering at 1735 °C for 22 h.

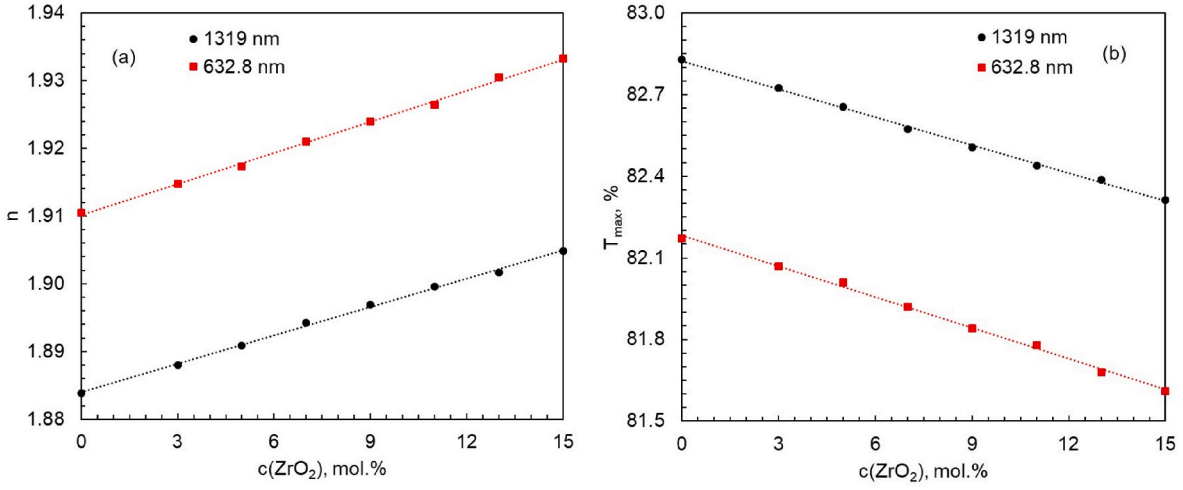

Fig. 6. Refractive index (n) of ZrO_2-doped Y_2O_3 ceramics vs. the ZrO_2 concentration at 632.8 and 1319 nm (a); theoretical in-line transmittance (T_{max}) at 632.8 and 1319 nm (b).

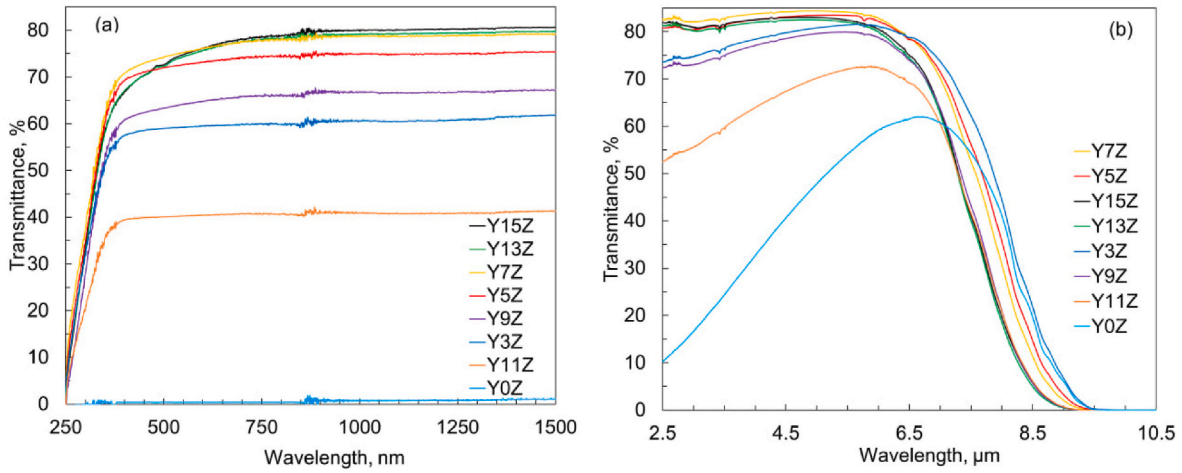

Fig. 8. In-line transmittance of 2-mm thick Y_2O_3 ceramics doped with different concentrations of ZrO_2 obtained by vacuum sintering at 1735 °C for 22 h: (a) in the UV-NIR range; (b) in the IR range. Captions to curves are arranged in order of transmittance decrease.

It was shown that the Vickers microhardness of Y_2O_3 ceramics doped with 3–15 mol.% of ZrO_2 increases with the doping concentration and reaches 10.3 GPa for 15 mol.% ZrO_2-doped yttria. Y_2O_3 ceramics doped with 15 mol.% of ZrO_2 possess also the highest transmittance in the visible-near IR wavelength ranges (77 % at 633 nm, 80.4 % at 1319 nm). It seems that a higher concentration of sintering aid is required for relatively low sintering temperature to obtain fully dense yttria ceramics. On the other hand, Y5Z and Y7Z ceramics demonstrate excellent transparency in the first atmospheric window (3–5 μm) and may be of great interest, taking into account their higher thermal conductivity [32].

CRediT authorship contribution statement

Dariia Chernomorets: Writing – review & editing, Writing – original draft, Validation, Project administration, Investigation, Conceptualization. **Pietro Galizia:** Investigation, Formal analysis. **Giacomo Zanetti:** Investigation. **Stefano Varas:** Investigation. **Alessandro Chiasera:** Investigation. **Andreana Piancastelli:** Investigation. **Roman Yavetskiy:** Writing – review & editing, Validation, Supervision, Conceptualization. **Jan Hostaša:** Writing – review & editing, Validation, Supervision, Resources, Project administration, Funding acquisition, Conceptualization.

Declaration of competing interest

The authors declare that they have no known competing financial interests or personal relationships that could have appeared to influence the work reported in this paper.

References

[1] L. Zhang, J. Yang, H. Yu, W. Pan, High performance of La-doped Y_2O_3 transparent ceramics, J. Adv. Ceram. 9 (2020) 493–502, https://doi.org/10.1007/s40145-020-0392-7.

[2] Q. Li, Y. Wang, J. Wang, J. Ma, M. Ni, H. Lin, J. Zhang, P. Liu, X. Xu, D. Tang, High transparency Pr:Y_2O_3 ceramics: a promising gain medium for red emission solid-state lasers, J. Adv. Ceram. 11 (2022) 874–881, https://doi.org/10.1007/s40145-022-0579-1.

[3] S.P. David, V. Jambunathan, F. Yue, A. Lucianetti, T. Mocek, Efficient diode pumped Yb:Y_2O_3 cryogenic laser, Appl. Phys. B 125 (2019), https://doi.org/10.1007/s00340-019-7250-8.

[4] J. Kong, D.Y. Tang, J. Lu, K. Ueda, Spectral characteristics of a Yb-doped Y_2O_3 ceramic laser, Appl. Phys. B 79 (2004) 449–455, https://doi.org/10.1007/s00340-004-1594-3.

[5] D.C. Harris, L.R. Cambrea, L.F. Johnson, R.T. Seaver, M. Baronowski, R. Gentilman, C. Scott Nordahl, T. Gattuso, S. Silberstein, P. Rogan, T. Hartnett, B. Zelinski, W. Sunne, E. Fest, W. Howard Poisl, C.B. Willingham, G. Turri, C. Warren, M. Bass, D.E. Zelmon, S.M. Goodrich, Properties of an infrared-transparent MgO:Y_2O_3 nanocomposite, J. Am. Ceram. Soc. 96 (2013) 3828–3835, https://doi.org/10.1111/jace.12589.

[6] Z. Xiao, S. Yu, Y. Li, S. Ruan, L.B. Kong, Q. Huang, Z. Huang, K. Zhou, H. Su, Z. Yao, W. Que, Y. Liu, T. Zhang, J. Wang, P. Liu, D. Shen, M. Allix, J. Zhang, D. Tang, Materials development and potential applications of transparent ceramics: a review, Mater. Sci. Eng. R Rep. 139 (2020) 100518, https://doi.org/10.1016/j.mser.2019.100518.

[7] A.L. Micheli, D.F. Dungan, J.V. Mantese, High-density yttria for practical ceramic applications, J. Am. Ceram. Soc. 75 (1992) 709–711, https://doi.org/10.1111/j.1151-2916.1992.tb07863.x.

[8] J. Iwasawa, R. Nishimizu, M. Tokita, M. Kiyohara, K. Uematsu, Plasma-resistant dense yttrium oxide film prepared by aerosol deposition process, J. Am. Ceram. Soc. 90 (2007) 2327–2332, https://doi.org/10.1111/j.1551-2916.2007.01738.x.

[9] D.C. Harris, Materials for Infrared windows and Domes, SPIE - The International Society for Optical Engineering, Washington, 1999, p. 415.

[10] R. Boulesteix, A. Maître, L. Chrétien, Y. Rabinovitch, C. Sallé, Microstructural evolution during vacuum sintering of yttrium aluminum garnet transparent ceramics: toward the origin of residual porosity affecting the transparency, J. Am. Ceram. Soc. 96 (2013) 1724–1731, https://doi.org/10.1111/jace.12315.

[11] A. Ikesue, K. Yoshida, Scattering in polycrystalline Nd:YAG lasers, J. Am. Ceram. Soc. 81 (1998) 2194–2196, https://doi.org/10.1111/j.1551-2916.1998.tb02607.x.

[12] S. Hříbalová, W. Pabst, Modeling light scattering by spherical pores for calculating the transmittance of transparent ceramics – all you need to know, J. Eur. Ceram. Soc. 41 (2021) 2169–2192, https://doi.org/10.1016/J.JEURCERAMSOC.2020.11.046.

[13] P. Colombo, Materials science: in praise of pores, Science 322 (2008) 381–383, https://doi.org/10.1126/science.1162962.

[14] J. Hostaša, F. Picelli, S. Hříbalová, V. Nečina, Sintering aids, their role and behaviour in the production of transparent ceramics, Open Ceram 7 (2021), https://doi.org/10.1016/j.oceram.2021.100137.

[15] C. Zhang, D. Ruan, Z. Tang, K. Lu, X. Wang, J. Qi, Z. Liao, T. Lu, Fabrication and luminescent properties of uranium doped Y_2O_3 transparent ceramics by sintering aid combinations, Opt. Mater. 125 (2022), https://doi.org/10.1016/j.optmat.2022.112064.

[16] L. Jin, G. Zhou, S. Shimai, J. Zhang, S. Wang, ZrO2-doped Y_2O_3 transparent ceramics via slip casting and vacuum sintering, J. Eur. Ceram. Soc. 30 (2010) 2139–2143, https://doi.org/10.1016/J.JEURCERAMSOC.2010.04.004.

[17] K. Ning, J. Wang, D. Luo, J. Zhang, Z.L. Dong, L.B. Kong, D.Y. Tang, New double-sintering aid for fabrication of highly transparent ytterbium-doped yttria ceramics, J. Eur. Ceram. Soc. 36 (2016) 253–256, https://doi.org/10.1016/j.jeurceramsoc.2015.09.007.

[18] X. Hou, S. Zhou, Y. Li, W. Li, Effect of ZrO_2 on the sinterability and spectral properties of $(Yb_{0.05}Y_{0.95})_2O_3$ transparent ceramic, Opt. Mater. 32 (2010) 920–923, https://doi.org/10.1016/j.optmat.2010.01.024.

[19] R.P. Yavetskiy, A.E. Balabanov, S.V. Parkhomenko, O.S. Kryzhanovska, A. G. Doroshenko, P.V. Mateychenko, A.V. Tolmachev, J. Li, N. Jiang, L. Gheorghe, M. Enculescu, Effect of starting materials and sintering temperature on microstructure and optical properties of Y_2O_3:Yb^{3+} 5 at% transparent ceramics, J. Adv. Ceram. 10 (2021) 49–61, https://doi.org/10.1007/s40145-020-0416-3.

[20] D.G. Chernomorets, O.S. Kryzhanovska, N.A. Safronova, A.E. Balabanov, A. G. Doroshenko, I.O. Vorona, S.V. Parkhomenko, A.V. Tolmachev, R.P. Yavetskiy, Optimization of rheological properties of Y_2O_3 slurries for obtaining IR-transparent ceramics, Met. Funct. Mater. 29 (2022) 244–251, https://doi.org/10.15407/fm29.02.244.

[21] H.M. Oh, H.N. Kim, Y.J. Park, J.W. Ko, H.K. Lee, Influence of starting Y_2O_3 and Nd_2O_3 powders characteristics on optical properties of highly transparent Nd:Y_2O_3 ceramics, Opt. Mater. 121 (2021) 111562, https://doi.org/10.1016/j.optmat.2021.111562.

[22] L. Gan, Y.J. Park, L.L. Zhu, H.N. Kim, J.W. Ko, J.W. Lee, Highly transparent Nd-doped yttria ceramics fabricated by hot pressing with ZrO_2 and La_2O_3 as sintering additives, J. Alloys Compd. 763 (2018) 192–198, https://doi.org/10.1016/j.jallcom.2018.05.304.
[23] P.L. Chen, I.W. Chen, Grain boundary mobility in Y_2O_3: defect mechanism and dopant effects, J. Am. Ceram. Soc. 79 (1996) 1801–1809, https://doi.org/10.1111/J.1151-2916.1996.TB07998.X.
[24] M. Ahsanzadeh-Vadeqani, R.S. Razavi, Spark plasma sintering of zirconia-doped yttria ceramic and evaluation of the microstructure and optical properties, Ceram. Int. 42 (2016) 18931–18936, https://doi.org/10.1016/j.ceramint.2016.09.043.
[25] R.S. Kumar, K.H.S. Priyanka, A.K. Khanra, R. Johnson, A novel approach of synthesizing nano Y_2O_3 powders for the fabrication of submicron IR transparent ceramics, Ceram. Int. 47 (2021) 16986–16999, https://doi.org/10.1016/J.CERAMINT.2021.02.270.
[26] L. Gan, Y.J. Park, L.L. Zhu, S. Il Go, H. Kim, J.M. Kim, J.W. Ko, Fabrication and properties of La_2O_3-doped transparent yttria ceramics by hot-pressing sintering, J. Alloys Compd. 695 (2017) 2142–2148, https://doi.org/10.1016/j.jallcom.2016.11.059.
[27] Y. Xu, X. Mao, J. Fan, X. Li, M. Feng, B. Jiang, F. Lei, L. Zhang, Fabrication of transparent yttria ceramics by alcoholic slip-casting, Ceram. Int. 43 (2017) 8839–8844, https://doi.org/10.1016/j.ceramint.2017.04.017.
[28] Y. Cao, H. Li, X. Zheng, S. Wang, C. Zhou, S. Chen, P. Yang, T. Zhou, H. Chen, L. Zhang, Simultaneous precipitation of Zr^{4+} and Y^{3+} ions induced refinement of precursors and powders in fabrication of Zr^{4+} doped Y_2O_3 transparent ceramics, Opt. Mater. 139 (2023), https://doi.org/10.1016/j.optmat.2023.113802.
[29] X. Li, X. Mao, M. Feng, J. Xie, B. Jiang, L. Zhang, Optical absorption and mechanism of vacuum-sintered ZrO_2-doped Y_2O_3 ceramics, J. Eur. Ceram. Soc. 36 (2016) 4181–4184, https://doi.org/10.1016/J.JEURCERAMSOC.2016.05.046.
[30] W. Liu, L. Jin, S. Wang, Preparation of ZrO2-doped Nd^{3+}:Y_2O_3 transparent ceramic and the corresponding characteristic of luminescence, Mater. Chem. Phys. 236 (2019), https://doi.org/10.1016/j.matchemphys.2019.121835.
[31] L.L. Zhu, Y.J. Park, L. Gan, S. Il Go, H.N. Kim, J.M. Kim, J.W. Ko, Effects of the Zr concentration on transparent Y_2O_3 ceramics fabricated by vacuum pre-sintering and a subsequent HIP treatment, J. Mater. Sci. Mater. Electron. 28 (2017) 7854–7861, https://doi.org/10.1007/s10854-017-6482-9.
[32] X. Li, Y. Xu, X. Mao, Q. Zhu, J. Xie, M. Feng, B. Jiang, L. Zhang, Investigation of optical, mechanical, and thermal properties of ZrO_2-doped Y_2O_3 transparent ceramics fabricated by HIP, Ceram. Int. 44 (2018) 1362–1369, https://doi.org/10.1016/j.ceramint.2017.08.204.
[33] Z. Yousefian, G. Dini, M. Milani, E. Arastoo, Zirconia-doped yttria transparent ceramics via slip casting and sintering, Mater. Chem. Phys. 273 (2021) 125097, https://doi.org/10.1016/j.matchemphys.2021.125097.
[34] X. Hou, S. Zhou, W. Li, Y. Li, Study on the effect and mechanism of zirconia on the sinterability of yttria transparent ceramic, J. Eur. Ceram. Soc. 30 (2010) 3125–3129, https://doi.org/10.1016/j.jeurceramsoc.2010.07.008.
[35] O. Fabrichnaya, F. Aldinger, Assessment of thermodynamic parameters in the system ZrO_2-Y_2O_3-Al_2O_3, Z. Metallkd. 95 (2004) 27–39, https://doi.org/10.3139/146.017909.
[36] D.G. Chernomorets, A. Piancastelli, L. Esposito, J. Hostaša, Effect of milling parameters on the morphology and sinterability of the yttrium oxide powders for transparent ceramics, Open Ceram 15 (2023), https://doi.org/10.1016/j.oceram.2023.100391.
[37] ASTM International, Standard test methods for apparent porosity, water absorption, apparent specific gravity. Bulk Density of Burned Refractory Brick and Shapes by Boiling Water, 2015, https://doi.org/10.1520/C0020-00R15.
[38] B.H. Toby, R.B. Von Dreele, GSAS-II: the genesis of a modern open-source all purpose crystallography software package, J. Appl. Crystallogr. 46 (2013) 544–549, https://doi.org/10.1107/S0021889813003531.
[39] A.P. Patel, C.R. Stanek, M.R. Levy, A. Chroneos, R.W. Grimes, Defect volumes of BO_2 doped Y_2O_3 (B = Ti, Zr, Hf and Ce), Nucl. Instrum. Methods Phys. Res. B 268 (2010) 3111–3113, https://doi.org/10.1016/j.nimb.2010.05.065.
[40] Q. Yi, S. Zhou, H. Teng, H. Lin, X. Hou, T. Jia, Structural and optical properties of Tm:Y_2O_3 transparent ceramic with La_2O_3, ZrO_2 as composite sintering aid, J. Eur. Ceram. Soc. 32 (2012) 381–388, https://doi.org/10.1016/j.jeurceramsoc.2011.09.015.
[41] H. Yoshida, M. Kodo, K. Soga, T. Yamamoto, Doping effect on sinterability of polycrystalline yttria: from the viewpoint of cation diffusivity, J. Eur. Ceram. Soc. 32 (2012) 3103–3114, https://doi.org/10.1016/j.jeurceramsoc.2012.04.010.
[42] Y. Xin, T. Xu, Y. Wang, P. Luo, W. Li, B. Kang, B. Mei, W. Jing, Effect of ZrO_2 content on microstructure evolution and sintering properties of $(Tb_{0.7}Lu_{0.3})_2O_3$ magneto-optic transparent ceramics, Magnetochemistry 8 (2022), https://doi.org/10.3390/magnetochemistry8120175.
[43] V.C. Stubican, R.C. Hank, S.P. Ray, Phase equilibria and ordering in the system ZrO_2-Y_2O_3, J. Am. Ceram. Soc. 61 (1978) 17–21.
[44] P. Duwez, F.H. Brown, F. Odell, The zirconia-yttria system, J. Electrochem. Soc. 98 (1951) 356–362.
[45] F.A. Kröger, H.J. Vink, Solid State Physics – Advances in Research and Applications, Academic Press, New York, 1957.
[46] L. Smrčok, Rietveld refinement of Y_2O_3 using the pearson VII profile shape function, I Cryst. Res. Technol. 24 (1989) 607–611.
[47] G. Baldinozzi, J.F. Bérar, G. Calvarin-Amiri, Rietveld refinement of two-phase Zr-doped Y_2O_3, Mater. Sci. Forum 278–281 (1998) 680–685. https://doi.org/10.4028/www.scientific.net/msf.278-281.680.
[48] M. Boniecki, Z. Librant, A. Wajler, W. Wesołowski, H. Weglarz, Fracture toughness, strength and creep of transparent ceramics at high temperature, Ceram. Int. 38 (2012) 4517–4524, https://doi.org/10.1016/j.ceramint.2012.02.028.
[49] H. Wang, Z. Huang, J. Qi, J. Wang, A new methodology to obtain the fracture toughness of YAG transparent ceramics, J. Adv. Ceram. 8 (2019) 418–426, https://doi.org/10.1007/s40145-019-0324-6.
[50] J.P. Hirth, J. Lothe, Theory of Dislocations, second ed., Krieger Publishing Company, New York, 1982.
[51] Y. Nigara, Measurement of the optical constants of yttrium oxide, Jpn. J. Appl. Phys. 7 (1968) 404, https://doi.org/10.1143/jjap.7.404.
[52] D.L. Wood, K. Nassau, Refractive index of cubic zirconia stabilized with yttria, Appl. Opt. 21 (1982) 2978–2981. https://10.1364/AO.21.0029781982.